Evaluation of the infant spine by direct sagittal computed tomography.

N Altman, D C Harwood-Nash, C R Fitz, S H Chuang and D Armstrong

AJNR Am J Neuroradiol 1985, 6 (1) 65-69
http://www.ajnr.org/content/6/1/65

Evaluation of the Infant Spine by Direct Sagittal Computed Tomography

Nolan Altman[1,2]
Derek C. Harwood-Nash[1]
Charles R. Fitz[1]
Sylvester H. Chuang[1]
Derek Armstrong[1]

Direct sagittal computed tomography (CT) and metrizamide myelography, in addition to standard axial CT, have proven most useful in evaluation of complex anomalies of the infant spine. Direct sagittal CT was performed by placing the entire infant sideways and supine within the gantry after metrizamide was injected. This technique was performed in six infants with diagnoses of lipoma with dysraphism, lipomyelomeningocele, lipomyelocystocele, lumbosacral agenesis with cord regression, capillary hemangioma, and vertebral osteomyelitis. The technique showed the relation and/or extension of lesions in the dorsal ventral plane, particularly the presence or absence of subarachnoid, enteric, or genitourinary communication. Spinal and paraspinal anatomic detail was also demonstrated beautifully.

Direct sagittal computed tomography (CT) as an adjunct to standard axial CT has been used successfully in the evaluation of the head [1–4]. In children in whom a complex spinal or paraspinal anomaly is demonstrated clinically, we have found that direct sagittal scanning of the spine after metrizamide myelography, with or without intravenous contrast enhancement, is a most valuable addition to conventional axial CT. Our aim was to improve the quality of the images and the accuracy of the diagnosis and to reduce the time of the CT examination and the number of axial cuts.

Technique

After lumbar puncture with injection of metrizamide, a standard myelogram was obtained under general anesthesia according to our usual practice [5]. Direct sagittal CT scans were obtained with a GE 9800 scanner by placing the entire infant sideways and supine within the gantry (fig. 1). The 48 cm scanning circle was used. This technique was limited to infants weighing about 6 kg or less, depending on their length and the gantry size. Consecutive sagittal 3 mm images were obtained with 2 sec scanning times at 120 kV and 100–140 mA after the midline was localized. Lower exposures to reduce radiation resulted in inferior images. The procedure is rapid; at most, six slices were sufficient to cover the spine and paraspinal regions in these small infants. Selective targeting for bone and/or soft tissue was performed using a 512 × 512 matrix. Standard axial CT images about the site of clinical concern were then obtained in the routine manner. All examinations were combined with metrizamide myelography.

Subjects

Six patients from the Hospital for Sick Children illustrate the usefulness of this technique. Five were referred from the department of neurological surgery and one from the department of orthopedic surgery. Their ages ranged from several days to 11 weeks and they all weighed under 6 kg.

Received March 28, 1984; accepted after revision July 11, 1984.

[1] Department of Radiology, Hospital for Sick Children, 555 University Ave., Toronto, Ontario, Canada M5G 1X8. Address reprint requests to D. C. Harwood-Nash.

[2] Present address: Department of Radiology, Miami Children's Hospital, Miami, FL 33155.

AJNR **6:65–69, January/February 1985**
0195–6108/85/0601–0065 $00.00

Case 1: Lumbosacral Agenesis with Cord Regression (fig. 2)

An 11-week-old infant was born to a diabetic mother by cesarean section after fetal distress at 35 weeks gestation. At birth the infant had bilateral femoral fractures, anomalies of the lower spine, bilateral hydroceles, an abnormal bony pelvis, and urinary incontinence. The infant was able to move both legs. On physical examination no vertebral bodies were palpated below L2, and a soft mass was felt in this region. The left hip appeared dislocated, and there was limited motion of both hips. The muscular tone of the legs was wasted and hypotonic. No reflexes could be elicited. The etiology of the soft-tissue mass was unclear and clinically was thought to represent a meningocele or lipomeningocele.

Direct sagittal CT showed no vertebral bodies below L2. There was cord regression, with the cord ending at the T10–T11 level; the sac extended to the T12–L1 region. There was a midline soft-tissue mass with a large discrete collection of simple fatty tissue with the suitable attenuation coefficient of fat and not a lipomeningocele. No communication was seen between the subarachnoid space and this fatty mass.

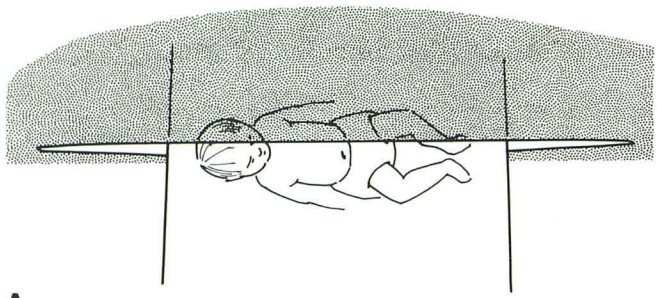

A

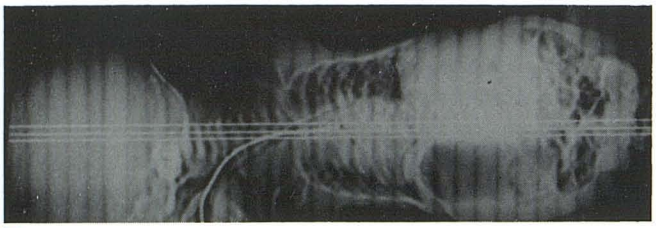

B

Fig. 1.—Positioning technique. **A,** Position of patient inside gantry for direct sagittal CT scanning. **B,** Scout view of patient in this position to localize midline and prescribe slice location.

Case 2: Lipomyelomeningocele (fig. 3)

A 37-week-gestation infant had multiple congenital anomalies at birth including exstrophy of the cloaca and bladder and omphalocele. The neurologic examination was normal, but there was a bilateral talipes equinovarus. A soft mass within the midbuttocks was palpated and diagnosed as a myelomeningocele. However, enteric communication was suspected and had to be excluded, along with a possible clear plane of cleavage between the myelomeningocele and the viscera.

In this very complex case the direct sagittal CT scan clearly identified the thickened filum entering a sacral meningocele; a more craniad placode with a myelocele was present and was surrounded by fat, and no bladder or enteric communication was accurately demonstrated. In addition a dysraphic spine was shown in the thoracic region.

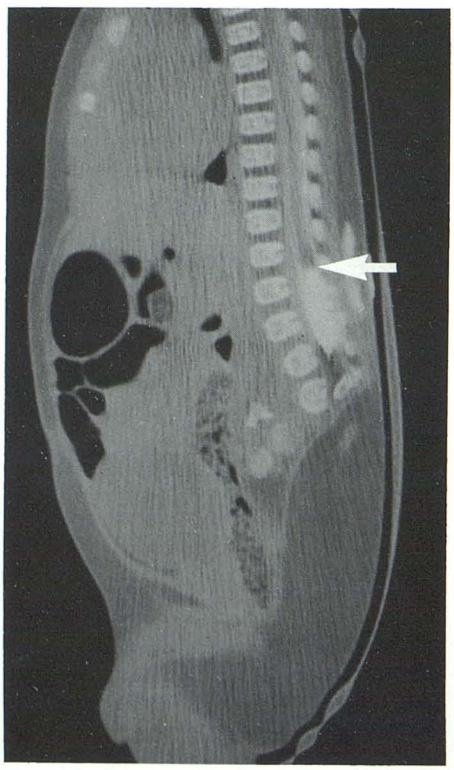

2

Fig. 2.—Case 1. Cord regression. Postmetrizamide direct sagittal CT scan. Absence of lumbar and sacral vertebrae below L2. Cord ends at T10–T11 (*arrow*) and sac at T12–L1. Caudal midline subcutaneous fatty mass is present without bowel, bladder, or central nervous system communication.

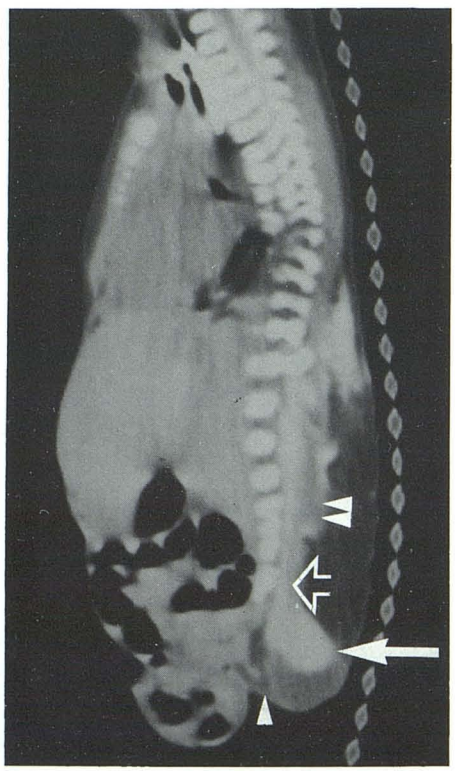

3

Fig. 3.—Case 2. Lipomyelomeningocele. Postmetrizamide direct sagittal CT scan. Dysraphism of lower thoracic and lumbosacral spine. Sacral meningocele (*closed arrow*), thickened filum (*open arrow*), and placode (*double arrowhead*). Anteriorly placed omphalocele and exstrophy of cloaca and bladder, which is completely separate from neurospinal anomalies with interposed discrete fatty layer (*single arrowhead*).

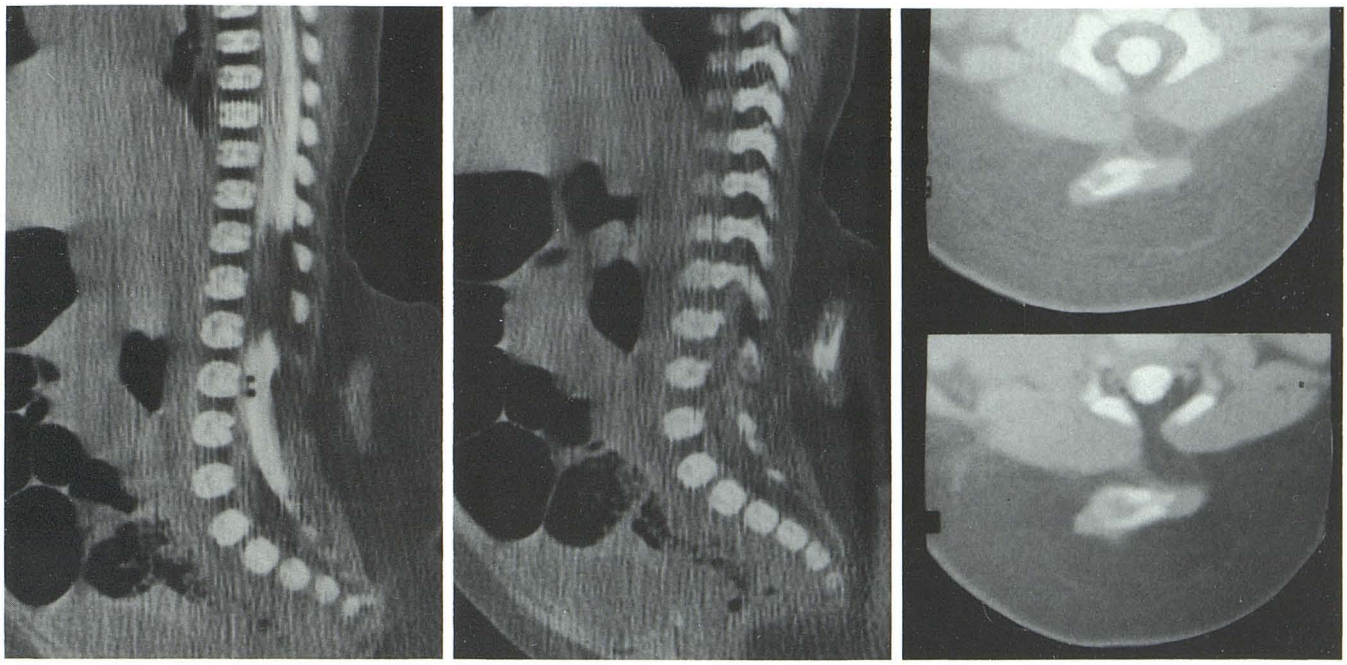

Fig. 4.—Case 3. Lipoma with dysraphism. **A,** Direct midline sagittal CT scan with metrizamide. Low cord merging with large, subcutaneous lipoma that blends through dura. **B,** Off-midline sagittal CT image. Density within lipoma consisting of aberrant cartilage and bone. **C,** Postmetrizamide axial images. Cartilage and bone within lipoma, which merges in these images with epidural fat. Continuation of fat into cord was not seen well on other axial images, and was best shown in **A.**

Fig. 5.—Case 4. Lipomyelocystocele. **A,** Selected postmetrizamide axial CT scan. Dysraphic spine, metrizamide-filled cyst, and posterior placode. **B,** Sagittal CT scan. Cord extending into sacrum expanding into cyst-myelocystocele with posterior placode and anteriorly coursing nerve roots. These features were definitively identified only postoperatively, and hence metrizamide must have been inserted directly into myelocystocele and nerve roots might have been simple strands contained within.

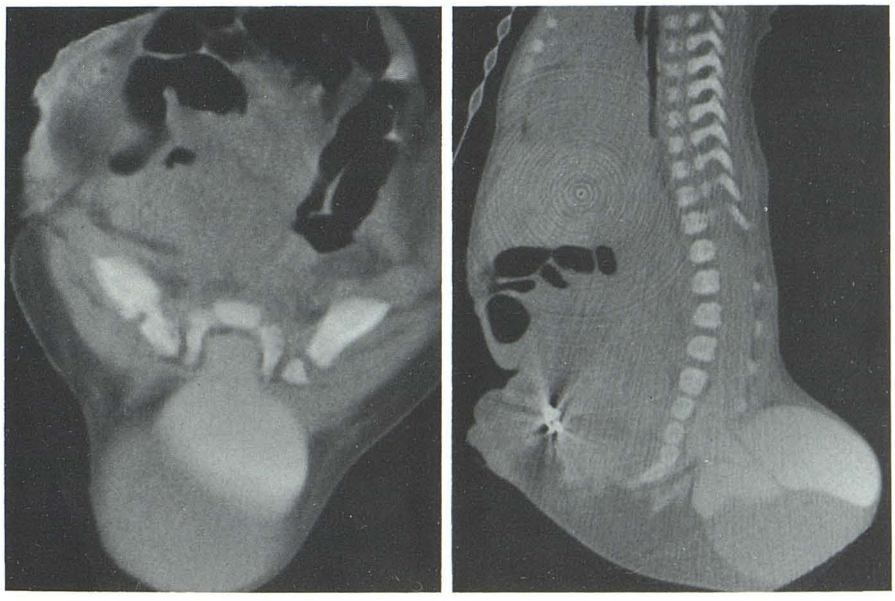

Case 3: Lipoma with Spinal Dysraphism (fig. 4)

A 1-month-old girl who was born uneventfully was noted to have a mass in her lower back. She moved both legs well and her bowel and bladder function were normal. It was believed that possible cord involvement by the lipoma was best evaluated with conventional CT axial images, and direct sagittal scans were obtained to assess their value vis-à-vis axial CT scans.

An extensive fatty mass entered the spinal cord, which was tethered low in the lumbar region. An area of increased density was noted within this fat and was believed to represent either bone or metrizamide. At surgery a 1 cm cleft in the dura was found with a large lipoma entering into the cord at the conus. This was subtotally removed, and at pathology a nidus of hyaline cartilage containing

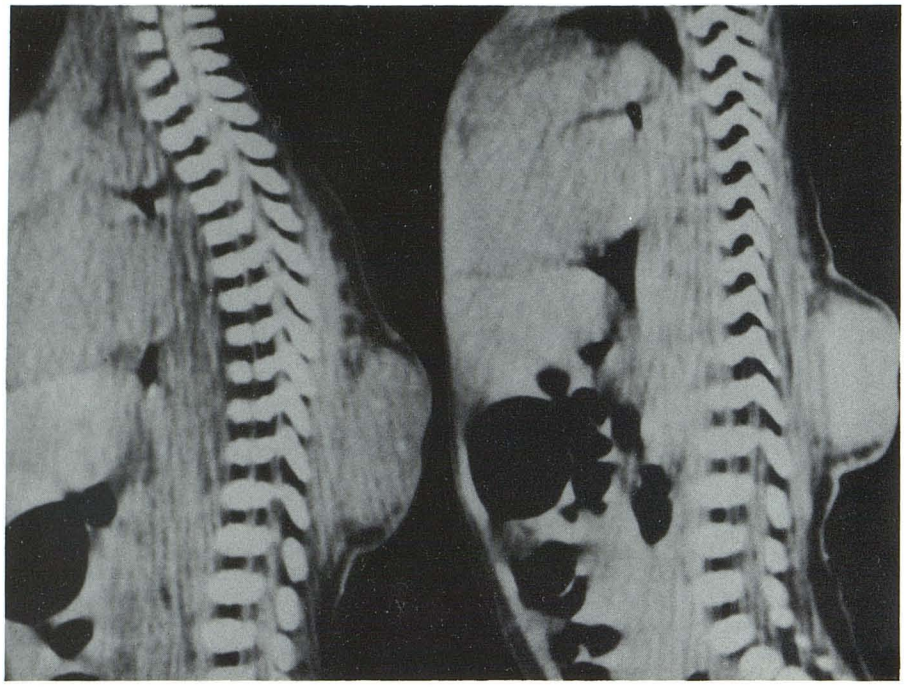

Fig. 6.—Case 5. Capillary hemangioma. Postmetrizamide direct sagittal CT scans before (*left*) and after (*right*) administration of contrast material. Large but discrete extraspinal hemangioma enhances.

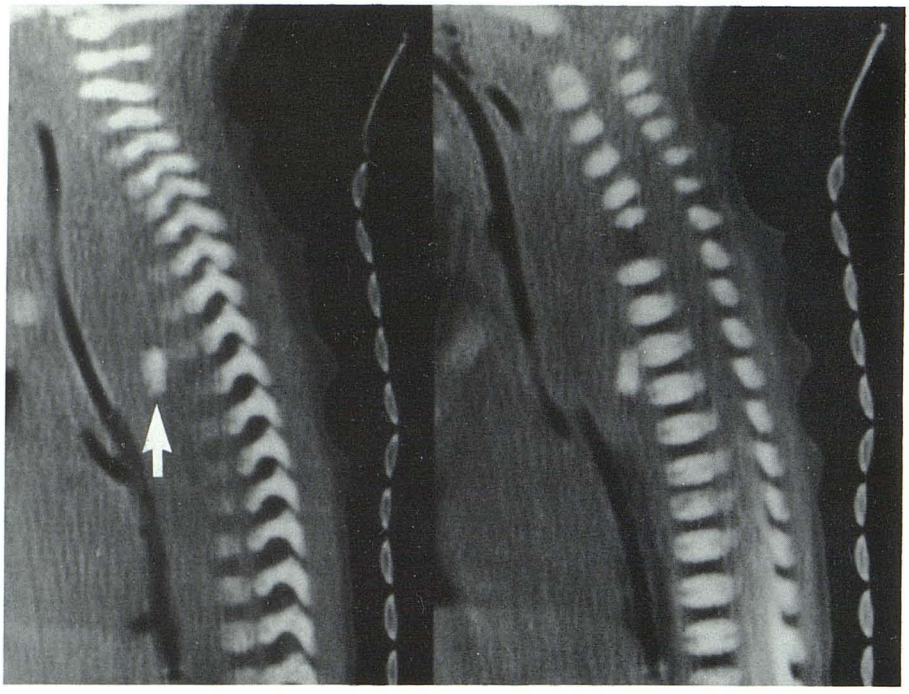

Fig. 7.—Case 6. Spinal osteomyelitis and posterior mediastinal abscess. Postmetrizamide direct sagittal CT scans off-midline (*left*) and midline (*right*). Large retrotracheal and esophageal abscess displacing these structures forward. Body of C7 (*arrow*) has floated free in pus and lies anterior to T3. Partial destruction of C6. Whole process is thought to have started as osteomyelitis of these vertebral bodies.

bone was found within the lipoma. Sagittal CT images proved to be superior to those in the axial plane.

Case 4: Lipomyelocystocele (fig. 5)

A 36-week-gestation infant was born prematurely with multiple congenital anomalies: omphalocele, bladder and cloacal exstrophy, imperforate anus, bifid scrotum, bilateral clubfeet, and an enlarging soft mass in the lower lumbar region. A meningocele with possible genitourinary and/or enteric communication was considered. This, together with the unusual increasing enlargement of the mass, prompted direct sagittal in addition to axial scans to best illustrate these complex relations.

The terminal part of the spinal cord was accurately shown to be distended with cerebrospinal fluid (CSF), hence a myelocystocele. A lipomatous placode was also noted inferiorly, and the nerve roots

were seen to extend ventrad across the dilated CSF-filled space. No communication with the enteric or genitourinary system was identified.

Case 5: Capillary Hemangioma (fig. 6)

A 1-week-old girl had a routine birth, but a large, raised, bluish mass was noted in the midline lumbar region. The rest of the physical examination was normal. Clinically this was believed to be a hemangioma; however, a central nervous system component or extension had to be excluded.

A direct sagittal CT scan with metrizamide, before and after intravenous injection of Hypaque 60, was obtained. This was done without anesthesia; axial images were not obtained. No communication with the subarachnoid space was easily demonstrated. Calcifications were present within the mass, which showed dense contrast enhancement. A diagnosis of a discrete capillary hemangioma was made. Clinical follow-up showed spontaneous regression with the only treatment being pressure applied externally.

Case 6: Osteomyelitis of the C7 Vertebra with a Perivertebral Abscess (fig. 7)

A 3-week-old girl was born uneventfully. She soon developed respiratory distress after a feeding, was taken to another hospital, required intubation, and was transferred to our institution. A chest film showed right-upper-lobe atelectasis. The white blood cell count was elevated. A swollen right knee was aspirated and grew out *Staphylococcus aureus*. The initial axial CT scan showed a mediastinal mass and a calcification within it. Plain films of the spine suggested an irregularity of the C7 vertebral body, but visualization of this region was difficult. A direct sagittal CT scan was obtained to better illustrate the lower cervical–upper thoracic vertebrae and the paravertebral region.

These direct sagittal CT scans showed absence of the C7 vertebral body and a paravertebral mass diagnosed as an abscess that pressed on the esophagus and trachea. An unusual calcified density within this abscess was considered to be an aberrant and separate C7 vertebral body. Additional partial destruction of C6 was also noted. Surgical exploration was performed from the right anterior lateral approach and the perivertebral abscess was drained. An ossified vertebral body was retrieved. The postoperative sagittal CT scan showed marked reduction in the size of the paravertebral abscess.

Discussion

In the evaluation of the neonatal spine, spinal cord, and paraspinal region, particularly in infants with complex spinal anomalies and dorsal masses, this technique of direct sagittal CT has proved most helpful. Direct CT images show better detail than those obtained by sagittal reformatting of axial CT images, as has been reported in direct versus reformatted coronal spinal CT [6]. Our technique will reduce the number of, or may obviate additional, axial images, thus reducing radiation exposure. It also provides better anatomic detail in the paraspinal region. The relation and/or extension of lesions, particularly the dorsal masses into the subarachnoid space, and the presence or absence of enteric or genitourinary communication are demonstrated beautifully. Correlation with magnetic resonance images displayed in this presentation would be helpful also. The neurosurgical correlation is much better, as it is the topography in this plane to which the surgeon is accustomed.

The spectrum of spinal dysraphism, from lipoma to lipomyelomeningocele, has been demonstrated most accurately by sagittal images; thus, these complex anomalies were well identified presurgically and all had good surgical correlation. The etiology of the dorsal mass in both the case of the cord regression and capillary hemangioma was also elucidated by the technique. The case of osteomyelitis of the C7 vertebra showed the associated perivertebral abscess and displaced body of C7, which prompted surgery. This technique also offered an additional method to view the upper thoracic–lower cervical region, which can be difficult with plain radiography or axial CT.

In summary, this technique is fast, accurate, and a good adjunct to standard axial CT images. With further familiarity the need for axial images in certain instances may be reduced or eliminated with this method.

REFERENCES

1. Bluemn P. Direct sagittal (positional) computed tomography of the head. *Neuroradiology* **1982**;22:199–201
2. Haverling M, Johanson H, Ahren L. Approximate sagittal computer tomography of the sellar and suprasellar region. *Acta Radiol [Diagn]* (Stockh) **1978**;19:918–920
3. Mondello E, Savin A. Technical note. Direct sagittal computed tomography of the brain. *J Comput Assist Tomogr* **1979**;3:706–708
4. Osborn AG, Anderson RE. Direct sagittal computed tomographic scans of the face and paranasal sinuses. *Radiology* **1978**; 129:81–87
5. Pettersson H, Harwood-Nash DC. *CT and myelography of the spine and cord*. Berlin: Springer-Verlag, **1982**
6. Kaiser MC, Pettersson H, Harwood-Nash DC, Fitz CR, Armstrong E. Direct coronal CT of the spine in infants and children. *AJNR* **1981**;2:465–466